CrossMark

# Effect of Nesting in Laminates on the Through-Thickness Permeability of Woven Fabrics

Bo Yang[1] · Shilong Wang[1] · Yankai Wang[1]

**Abstract** The layer nesting phenomenon of multilayer fabric has a great influence on the through-thickness permeability, which is a key parameter for the simulation of the through-thickness LCM (Liquid Composite Moldling) processes. In this paper, based on the analyses of the formation reason and characterization parameters of layer nesting, the geometry models of fabric unit-cells with nesting are established. The through-thickness flow in the unit-cell is analyzed to built the governing equations of the resin flow. The inter-yarn and intra-yarn regions of the unit-cell model are discretized uniformly, then the governing equations of the through-thickness flow are numerically solved based on Adams-Bashforth scheme and Chorin projection method, so the through-thickness flow parameters is obtained and the through-thickness permeability of the fabric with nesting can be predicted. The verification of the above method is implemented by comparisons with the available experimental results. A series of simulation experiments are carried out to investigate the nesting behaviors under different layer shifts, and the effects of nesting on the total thickness and through-thickness permeability of woven fabric are researched in detail.

## 1 Introduction

Liquid composite molding (LCM) processes have been widely used in the manufacturing of complex composite structures, in those processes, a liquid resin is injected or sucked into a closed mold containing a multiaxial dry fiber preform to exclude air and infiltrate the preform. In general, resin flows on the in-plane direction to fill the pores in preform, such as the resin transfer molding (RTM) process, while the long flow distance and complicated flow path can easily lead to molding defects, such as void and dry spot. Therefore, the through-thickness

---

✉ Bo Yang
yangbo61@cqu.edu.cn

[1]  State Key Laboratory of Mechanical Transmission, Chongqing University, Chongqing, China

LCM processes, in which resin flows on the through-thickness direction such as resin infusion processes, are getting more attractive due to its advantages of low cost, short cycle and simple flow path. Same to other LCM processes, prediction of the filling time and optimization of the process parameters using numerical simulation technique are very necessary to the through-thickness LCM processes.

In the numerical simulation of the mold-filling stage in LCM, resin and preform are modeled as an incompressible viscous fluid and a porous medium, respectively. The flow parameters can be obtained by solving Darcy's law (Eq. (1)) and mass conservation equation (Eq. (2)) simultaneously using finite element method (FEM) or finite volume method (FVM) [1, 2]

$$\overline{\mathbf{u}} = -\frac{\mathbf{K}}{\mu} \cdot \nabla p \tag{1}$$

$$\nabla \cdot \mathbf{u} = 0 \tag{2}$$

where $\overline{u}$ is the volume averaged flow velocity of resin in the mould, $K$ is the permeability tensor of the preform, $\mu$ is the viscosity of the resin, and $p$ is the resin pressure.

The permeability tensor $K$ is an inherent characteristic related to the structural features of the preform. As a key input parameter, $K$ plays an important role on the accuracy of the mold-filling simulation results, it must be predicted precisely in advance. Many studies have been carried out on simulation predict and experiment measurement of the in-plane permeability of the woven fabrics [3–8]. However, there is a little literature on the through-thickness permeability, and most of them focused on the test measurement [9–13] and theoretical prediction model [14–16]. Markicevic et al. [14] proposed an explicit model for the through-thickness permeability of porous media comprised of alternating layers of tows of varying permeability, it allows calculation of the overall permeability from the permeabilities of the inter-yarn and intra-yarn regions, the validation of the model was carried out through CFD simulations. Xiao et al. [15] proposed an analytical model to predict through-thickness fabric permeability based on viscous and incompressible Hagen-Poiseuille flow. The key feature in the model is that a parabolic function was used within the Hagen–Poiseuille flow integration to capture the geometry of the flow channel formed by interwoven yarns. The accuracy of the model was verified by air permeability measurements. In addition, they also established an analytical model for through-thickness permeability prediction of 3D fabrics using a similar method [16]. Nabovati et al. [17] developed the simulation algorithm for fluid flow in complex geometries based on the lattice Boltzmann method (LBM), which was employed to investigate the through-thickness permeability of woven fabrics.

Before the mold-filling process, the preform with desired thickness is usually obtained by lay-up of woven fabric, nesting inevitably occurs between neighboring plies, which plays an important role in determining permeability of preform [18]. At present, many scholars have studied the influence of nesting on the in-plane permeability of textile preforms [19–21], while very little research has addressed the relationship of nesting to the through-thickness permeability. Fang et al. [22, 23] investigated the effect of nesting on the through-thickness permeability for the 0°/90° noncrimp fabrics and unidirectional fabrics, they decomposed the fabric unit cell into zones of characteristic yarn arrangement and predicted the through-thickness permeability of unidirectional fabrics by theoretical derivation. The experimental results showed that the permeability values are two orders of magnitude larger with minimum

nesting than those with maximum nesting. Song et al. [24] proposed an analytical model to analyze the effect of the number of preform layers on the through-thickness permeability from a statistical viewpoint.

As can be seen from the above analysis, at present, the through-thickness permeability of woven fabrics are usually predicted by theory analytic method, which is accomplished by simplification of fabric structure and equivalent of flow channel, so the effects of complicated nesting behaviors and degree on the through-thickness permeability of woven fabrics cannot be researched deeply. In this paper, the nesting behavior is analyzed and the geometry model of woven fabric with layer nesting is established firstly. Then the through-thickness resin flow behavior is analyzed, the numerical simulation of the resin flow is implemented based on finite-difference discretization of Brinkman equations, and then the prediction of the through-thickness permeability of woven fabrics is achieved. Comparisons with the available experimental results are made to verify the above method. At last, a series of simulation tests are carried out to investigate the nesting behaviors on different fabric layer shifts, and the effects of nesting on the total thickness and through-thickness permeability of woven fabric are researched in detail.

## 2 Layer Nesting and its Geometry Modeling

Layer nesting refers to the interaction between neighboring fabric layers of a textile composite laminate: because of the horizontal shift between neighboring fabric layers, yarns from one layer are situated in the valleys formed by yarns of the layer beneath it [18, 23]. Figure 1 shows a woven fabric and its geometry model, woven fabric is formed by interlacing of the warp and weft yarns. At the crossover points, the local fabric thickness is the sum of the thicknesses of the two yarns, which is called nominal thickness of the fabric $h$. While at the meso pores between yarns, the local fabric thickness is 0. It is because of the inhomogeneity of the local fabric thickness, the crossover points of a fabric layer may invade into the inter-yarn pores of the adjacent layer during ply stacking, which is layer nesting.
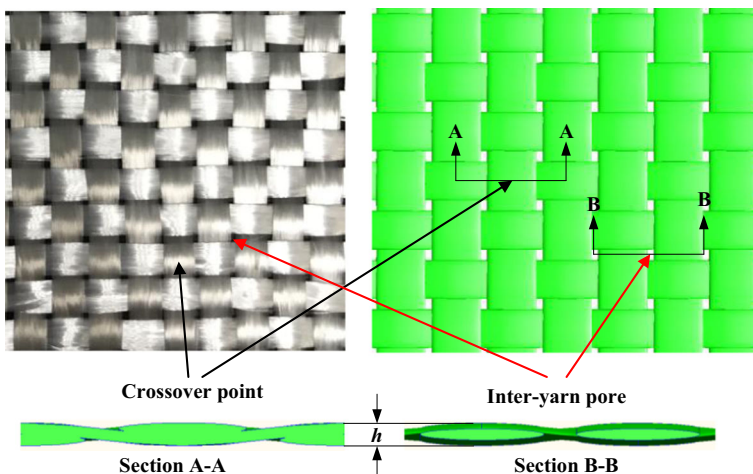


**Fig. 1** A woven fabric and its geometry model

Figure 2 shows the unit-cell models of dual-layer fabric with nesting, the coordinate system is shown in figures. In Fig. 2a, no in-plane relative shift occurs between the two layers, so the crossover points of the two layers contact to each other. In this situation, no layer nesting occurs (i.e. minimum nesting state), the total thickness $H = 2\,h$. In Fig. 2b, the fabric layers shift relative to each other, the crossover points of the upper layer are aligned to the inter-yarn pores of the lower layer. In this situation, the upper layer invades into the lower layer, layer nesting occurs, the total thickness $H < 2\,h$. In this figure, the relative shift distances on weft and warp directions ($x$ and $y$ directions) are $p_{we}/2$ and $p_{wa}/2$ respectively, the maximum nesting state appears, in this case, the total thickness $H$ is minimum. In actual conditions, random cases between minimum nesting and maximum nesting will occur since the random relative shift.

In this paper, the geometry model of the woven fabric with layer nesting is established by ACIS, the principle of minimum potential energy is used to compute the structure parameters of the fabric [18, 25].

## 3 Through-Thickness Flow and its Mathematical Model

The woven fabric is a porous medium contains two distinct scales of pores, intra-yarn pores (micron scale) and inter-yarn pores (millimeter scale). Therefore, the through-thickness flow in the fabric preform consists of inter-yarn flow and intra-yarn flow as shown in Fig. 3. The different scales of pores has different flow resistances, in inter-yarn pores, the flow resistance is little and the flow velocity is high, while in the intra-yarn pores, the flow resistance is large and the flow velocity is low. According to the figure, we can find that nesting will lead to the transformation of pores, which may affect the flow seriously.
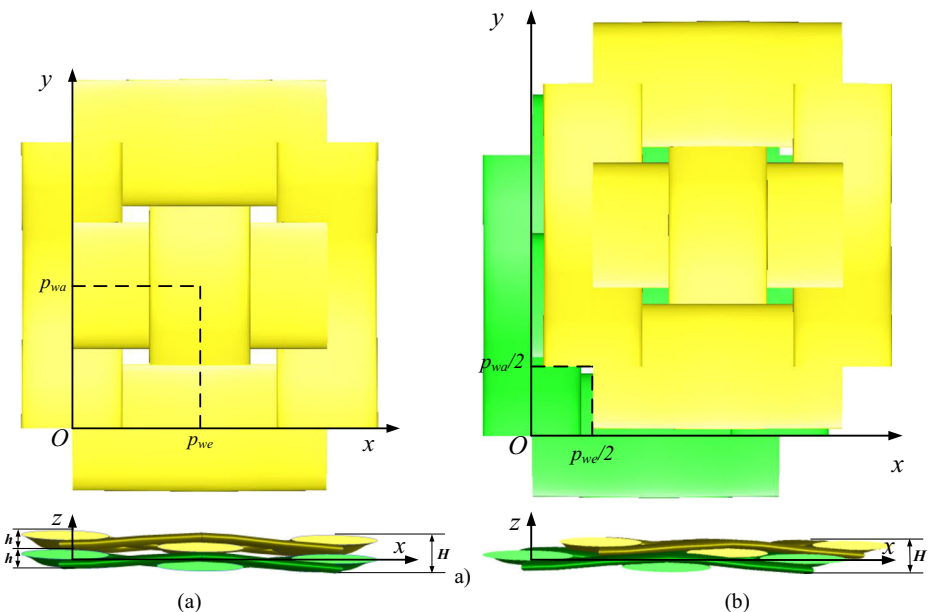


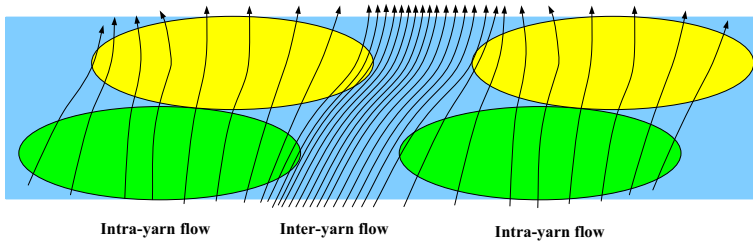Fig. 2 The unit-cell models of dual-layer fabric with nesting

**Fig. 3** The through-thickness flow in the fabric with nesting

During LCM, resin is usually modeled as an incompressible viscous fluid, the mold-filling process is seen as a creeping and isothermal flow, the inter-yarn flow can be described by Stokes equation [7, 8, 25]:

$$\frac{\partial \mathbf{u}}{\partial t} = -\nabla p + \mu \Delta \mathbf{u} \tag{3}$$

For the intra-yarn flow, we consider yarns as porous medium, Brinkman equation is used to describe the intra-yarn flow [7, 8]

$$\frac{\partial \mathbf{u}}{\partial t} + \frac{\mu \mathbf{u}}{\mathbf{K}_{\text{yarn}}} = -\nabla p + \mu \Delta \mathbf{u} \tag{4}$$

where $\mathbf{K}_{\text{yarn}}$ is the local permeability of the yarn, which is affected by the fiber distribution. $K_{\text{yarn}}$ can be obtained from Gebart model [26]:

$$
\begin{aligned}
k_{\text{along}} &= \frac{8}{53} \frac{(1-V_{\text{f}})^3}{V_{\text{f}}^2} r^2 \\
k_{\text{trans}} &= \frac{16}{9\pi\sqrt{6}} \left( \sqrt{\frac{V_{\text{fmax}}}{V_{\text{f}}}} - 1 \right)^{5/2} r^2
\end{aligned}
\tag{5}
$$

where $k_{\text{along}}$ and $k_{\text{trans}}$ indicate the permeability for flow parallel and transverse to the fiber direction, $V_{\text{f}}$ is the fiber volume fraction of yarn, $V_{\text{fmax}}$ is the maximal fiber volume fraction of the yarn, $r$ is the radius of the monofilament fiber.

As can be seen by comparing Eqs. (3) and (4), the Brinkman equation can be seen as an extension of Stokes equation, the additional term $\mu u/\mathbf{K}_{\text{yarn}}$ can be seen as a penalization of Eq. (3), so the inter-yarn flow can be expressed by the Brinkman equation with $1/\mathbf{K}_{\text{yarn}} = 0$.

# 4 Simulation Prediction of Through-Thickness Permeability for Woven Fabrics

The through-thickness permeability $K_z$ for woven fabrics can be obtained from the following equation according to Eq. (1),

$$K_z = -\frac{\mu \cdot \overline{u}_z}{dp/dz} \tag{6}$$

here $u_z$ is the flow velocity on the through-thickness direction.

Therefore, the velocity and pressure distributions of through-thickness flow need to be obtained to compute the through-thickness permeability. In this paper, Eqs. (4) and (2) are simultaneously solved by finite difference method (FDM) to obtain the through-thickness flow parameters in the dual-layer unit-cell of woven fabric with nesting, then the through-thickness permeability of the fabric can be predicted from Eq. (6).

The geometry discretization of the flow region is shown in Fig. 4, since both inter-yarn and intra-yarn regions are flow regions, they should be discretized uniformly. The local permeability of the yarn $\mathbf{K}_{yarn}$ needs to be assigned on the elements located in the intra-yarn regions, the affiliation of each element is judged by its center position as shown in Fig. 4. A dual-layer unit-cell of woven fabric with nesting is shown in Fig. 5a, it is the representative volume element (RVE) of the dual-layer fabric and will be used to predict the through-thickness permeability of the dual-layer fabric. Figure 5b shows the discrete model of the unit-cell, in which the blue elements locate in the inter-yarn region.

Before simulation, appropriate boundary conditions must be imposed on the boundary of the flow regions. On the through-thickness direction, constant pressure inlet and outlet are exerted on the top and bottom surfaces. On other directions, the periodic boundary condition is applied. In order to avoid the results of meaningless zigzag velocity and pressure distribution, the physical parameters of resin flow are arranged on a staggered grid as shown in Fig. 6. Pressure is computed on the black nodes, while horizontal and vertical velocities are computed on the gray and white nodes, respectively.

Since there is a large gap between the flow resistances of inter-yarn region and intra-yarn region, the velocity discontinuity will occur at the surface of yarn. If the normal finite-difference scheme is adopted, spurious numerical oscillations may appear, the stability of numerical calculation will be destroyed. In order to solve the above problem, the Adams-Bashforth scheme which satisfies the high resolution and total variation diminishing (TVD) conditions is employed for the time discretization in this article. Adams-Bashforth scheme is a one-step, three-layer, time forward difference scheme for the discretization of convection equation, its truncation error is $O(\Delta t^2, \Delta x^2)$ [27]. The Chorin projection method is applied to decouple the Brinkman equation and the continuity equation. The detailed solving algorithm and process have been discussed in Ref. [21].
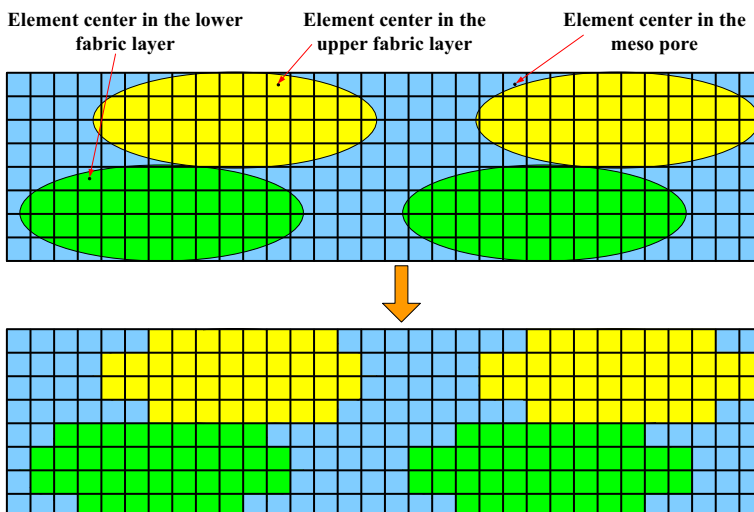


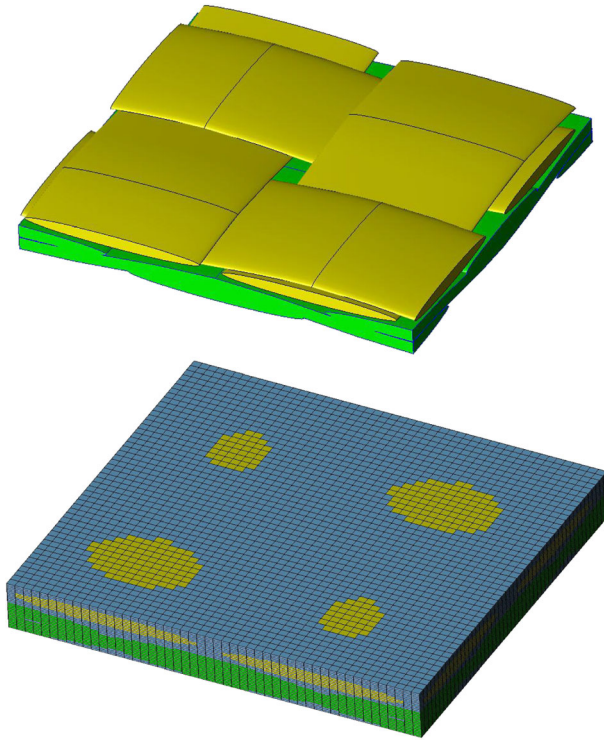**Fig. 4** The geometry discretization of the flow region

**Fig. 5** A dual-layer unit-cell of woven fabric with nesting and its discrete model
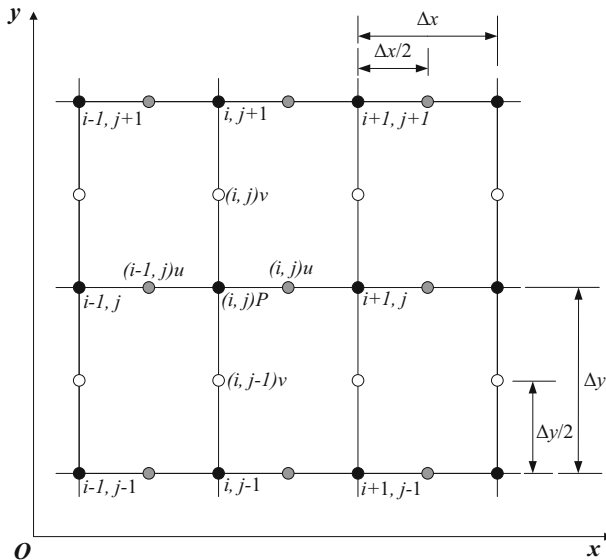


**Fig. 6** The staggered grid
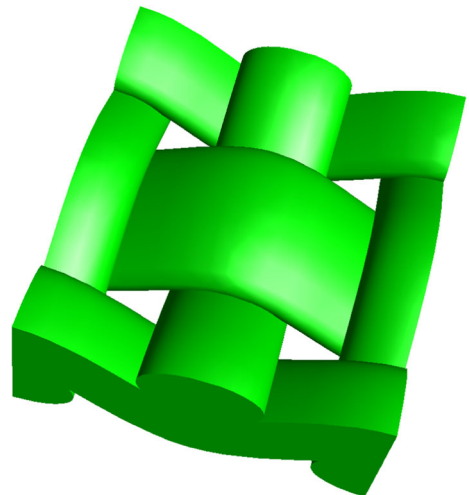
**Table 1** Geometry parameters of $U_1$ fabric

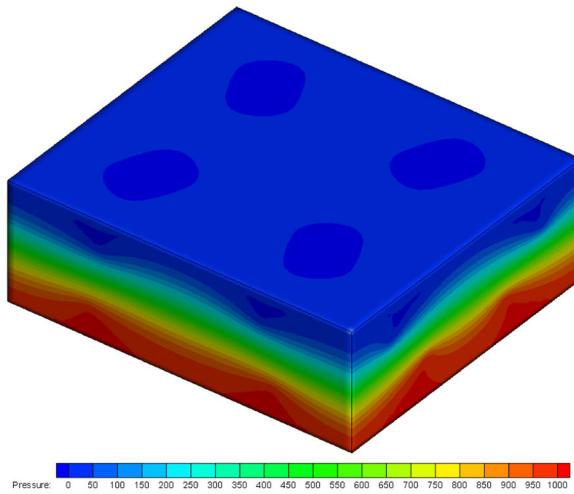| Description | Value |
| --- | --- |
| Width of the warp yarns/mm | 0.405 |
| $p_{wa}$/mm | 0.41 |
| Width of the weft yarns/mm | 0.279 |
| $p_{we}$/mm | 0.47 |
| Thickness/mm | 0.323 |

# 5 Experimental Verification

In order to verify the effectiveness of the above geometry modeling and simulation methods for through-thickness permeability prediction of woven fabric, the through-thickness permeability of single-layer $U_1$ plain woven fabric is predicted and is compared with experimental result. The geometry parameters of $U_1$ fabric are listed in Table 1 [15, 28], and Fig. 7 shows its unit-cell model.

The interval counts of the discrete model on $x$, $y$ and $z$ directions are 50, 50 and 30, respectively. The interval size of the through-thickness direction is smaller than other directions, which can improve the computational accuracy of through-thickness flow. The following parameters are applied in the simulation, inlet pressure $P_{in} = 1000$ Pa, outlet pressure $P_{out} = 0$ Pa, fluid viscosity $\mu = 0.2$ Pa·s. The average diameter of monofilament fibers is 8.6 μm, the fiber volume fraction of yarn is 0.56 [15], the longitudinal and transversal permeability values of yarn are $k_{along} = 7.581 \times 10^{-13}$ m$^2$ and $k_{trans} = 1.657 \times 10^{-13}$ m$^2$ according to Eq. (5). The simulation results of flow in unit-cell model of $U_1$ fabric are shown in Fig. 8. As can be seen from the figure, the through-thickness flow velocity in inter-yarn pores is significantly larger than that in intra-yarn pores, which is caused by the flow resistance difference. After volume averaging of flow velocity, the simulated through-thickness permeability of $U_1$ fabric is $1.53 \times 10^{-11}$ m$^2$ according to Eq. (6). The through-thickness permeability of single layer $U_1$ fabric was experimental measured in Ref. [15], the experimental result shows the through-thickness permeability of single layer $U_1$ fabric is $1.21 \times 10^{-11}$ m$^2$. Through comparison, we can find

**Fig. 7** The unit-cell model of single-layer U1 fabric

(a) Pressure distribution
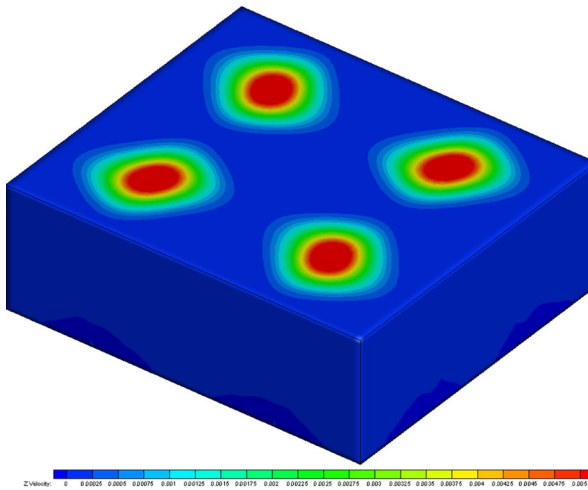


(b) Through-thickness velocity distribution

**Fig. 8** The simulation results of through-thickness flow in unit-cell of single-layer $U_1$ fabric

**Table 2** Geometry parameters of EWR600 fabric

| Description | Value |
| --- | --- |
| Width of the warp yarns/mm | 2.95 |
| $p_{wa}$/mm | 3.74 |
| Width of the weft yarns/mm | 3.24 |
| $p_{we}$/mm | 3.68 |
| Thickness/mm | 0.6 |

**Fig. 9** The unit-cell model of single-layer EWR600 fabric
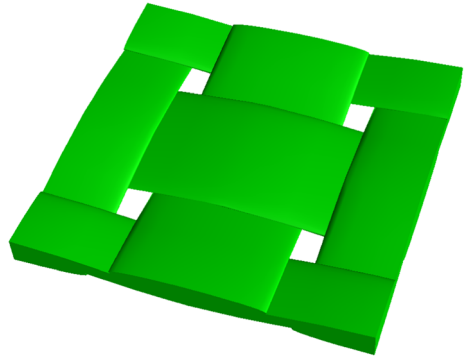


that the prediction result of the above method is close to the experimental result, the requirement of permeability prediction is satisfied [7, 29].

## 6 Effect of Layer Nesting on Through-Thickness Permeability

The dual-layer EWR600 plain woven fabric is employed to investigate the effect of layer nesting on through- thickness permeability. The geometry parameters of EWR600 fabric are listed in Table 2, and Fig. 9 shows its unit-cell model.

### 6.1 Unidirectional Shift

The coordinate system as shown in Fig. 10 is built for the dual-layer unit-cell of EWR600 woven fabric with nesting, $x$ and $y$ axis coincide with the axial directions of weft yarn and warp
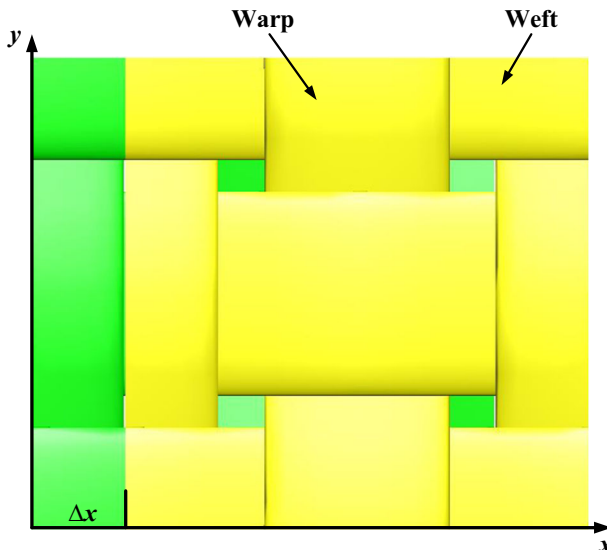


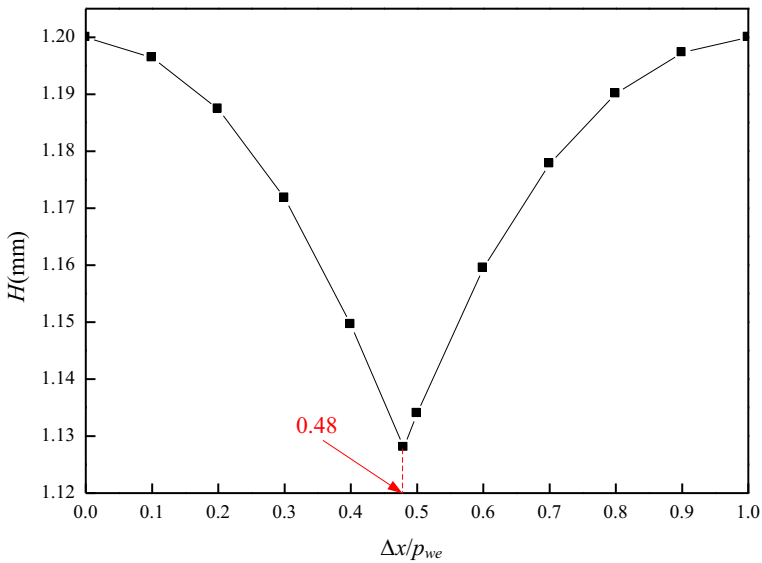**Fig. 10** The dual-layer unit-cell of EWR600 woven fabric with $x$-shift

**Fig. 11** The change rule of total thickness $H$ with $\Delta x$

yarn, and the relative shift distances on $x$ and $y$ axis are expressed by $\Delta x$ and $\Delta y$, respectively. Unidirectional shift means the relative shift of the two unit-cells occurs only on $x$ or $y$ direction, i.e. one of $\Delta x$ and $\Delta y$ is 0. The relative shift between the two unit-cells shown in Fig. 10 occurs only on $x$ direction, i.e. $\Delta x \neq 0$, $\Delta y = 0$.

Figure 11 shows the change rule of total thickness $H$ with $\Delta x$. Because of the structure symmetry of unit-cell, when $\Delta x = 2p_{we}$, the relative position of the upper and lower unit-cells is identical to the initial position, that means the shift period is $2p_{we}$, in a shift period, nesting behavior is symmetrical to $\Delta x = p_{we}$. Therefore, the total thickness and through-thickness permeability values when $0 < \Delta x < p_{we}$ are studied. From Fig. 11 we can find that with the
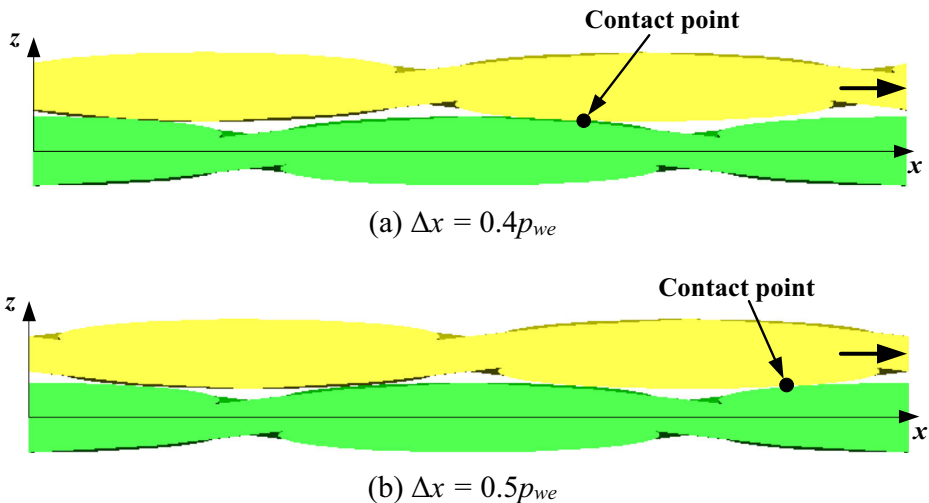


(a) $\Delta x = 0.4p_{we}$



(b) $\Delta x = 0.5p_{we}$

**Fig. 12** Switch of the superficial contact point between the two fabric unit-cells
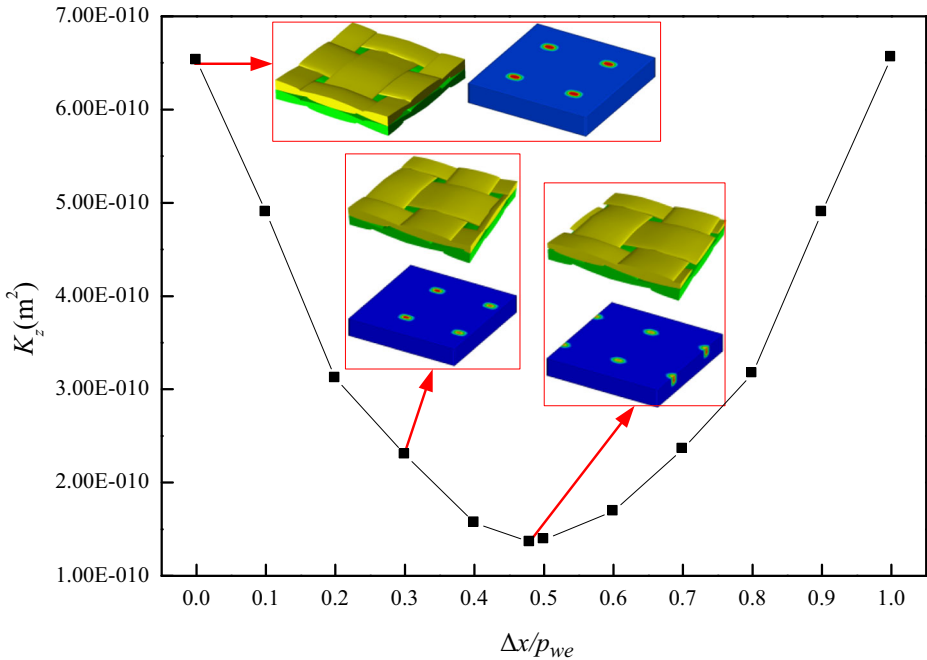
**Fig. 13** The change rule of through-thickness permeability $K_z$ with $\Delta x$

increase of shift distance $\Delta x$, the total thickness decreases firstly, $H$ reaches the minimum value at $\Delta x = 0.48p_{we}$. Thereafter, $H$ rises until it reaches the initial value 1.2 mm at $\Delta x = p_{we}$. The reason why the minimum total thickness occurs at $\Delta x = 0.48p_{we}$ instead of $\Delta x = 0.5p_{we}$, is because the superficial contact point between the two fabric unit-cells switches at $\Delta x = 0.48p_{we}$ as shown in Fig. 12. When $\Delta x$ is smaller than $0.48p_{we}$, the edge of yarn transverse section of the upper layer contacts with the edge of yarn longitudinal section of the lower layer as shown in Fig. 12a, when $\Delta x$ is bigger than $0.48p_{we}$, the edges of yarn transverse sections of the two layers contact with each other as shown in Fig. 12b. Since the edge of yarn transverse section and axis of yarn meet different curvilinear equations, the superficial contact point does not switch at $\Delta x = 0.5p_{we}$ exactly. We call the position of $\Delta x = 0.48p_{we}$ as the maximum nesting position of x-shift. According to Fig. 11, the change rate of total thickness is smaller at low nesting degree than that at high nesting degree, which is caused by the larger curvature of the contact point at high nesting degree.

Presented in Fig. 13 is the change of through-thickness permeability with the nesting degree. A change rule similar to the total thickness appears in Fig. 13, as the increase of $\Delta x$, the through-thickness permeability decreases firstly and then increases, at $\Delta x = 0.48p_{we}$, it reaches the minimum value. However, the change rate of through-thickness permeability shows a contrary tendency with the total thickness, the change rate of through-thickness permeability is bigger at low nesting degree than that at high nesting degree. According to the geometry models and velocity distributions of different nesting degrees, we can find that the locations of the inter-yarn pores change with the nesting degree, eventually leads to a major change of velocity distributions.

When the relative shift of the two unit-cells occurs only on x direction, the cross section of $y = 0.5p_{wa}$ has the maximal inter-yarn pores and the maximal through-thickness flow velocity.
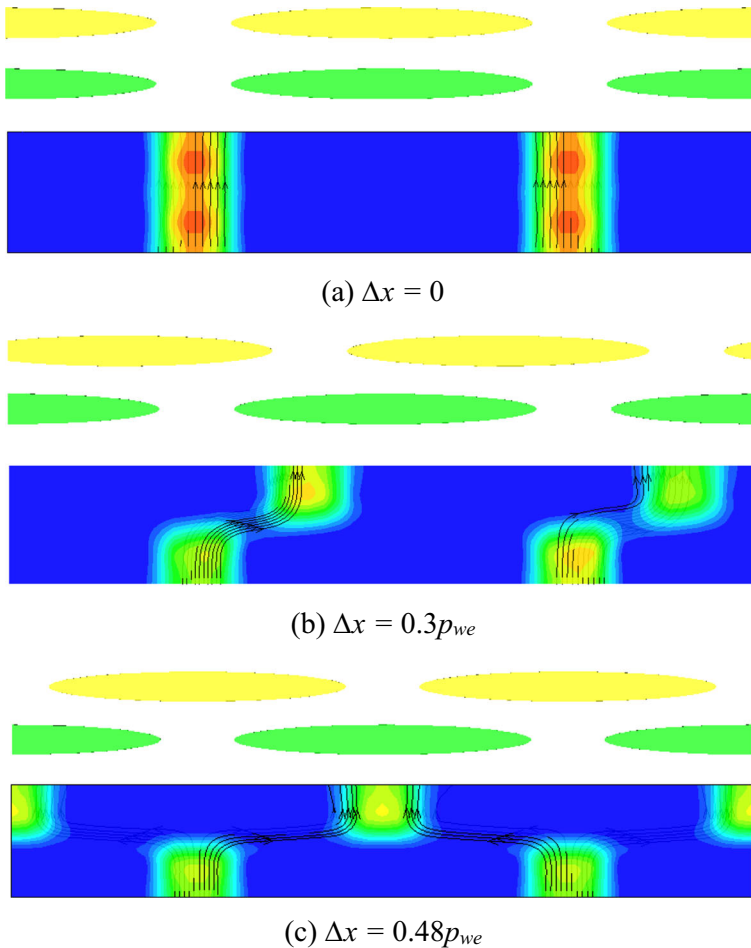
(a) $\Delta x = 0$



(b) $\Delta x = 0.3p_{we}$



(c) $\Delta x = 0.48p_{we}$

**Fig. 14** The variations of inter-pores and flow streamlines with the nesting degree

Figure 14 shows the variations of inter-pores and flow streamlines with the nesting degree. As can be seen from the figure, the two unit-cells do not contact to each other on the cross section of $y = 0.5p_{wa}$, so the connected inter-yarn pores are formed and become the main flow channel of resin. When $\Delta x = 0$, the inter-yarn pores of the upper and lower unit-cells are aligned to each other, the vertical main flow channels are formed as shown in Fig. 14a. The vertical main flow channels have large width and small length, so the velocity of inter-yarn flow is high. With the increase of $\Delta x$ which means the rise of nesting degree, the total thickness decreases, the length of main flow channel increases and the width decreases as shown in Fig. 14b, the two behaviors of the main flow channel result in the decrease of inter-yarn flow velocity and through-thickness permeability. When $\Delta x = 0.48p_{we}$, the width of the main flow channel and the through-thickness permeability reach the minimum. While when $\Delta x = 0.5p_{we}$, the length of main flow channel reaches the maximum, the value of through-thickness permeability increases a little as shown in Fig. 13. According to the above phenomenon, we can find that, compared to the length increase of the main flow channel, the width decrease is a more significant factor in reducing the through-thickness permeability.
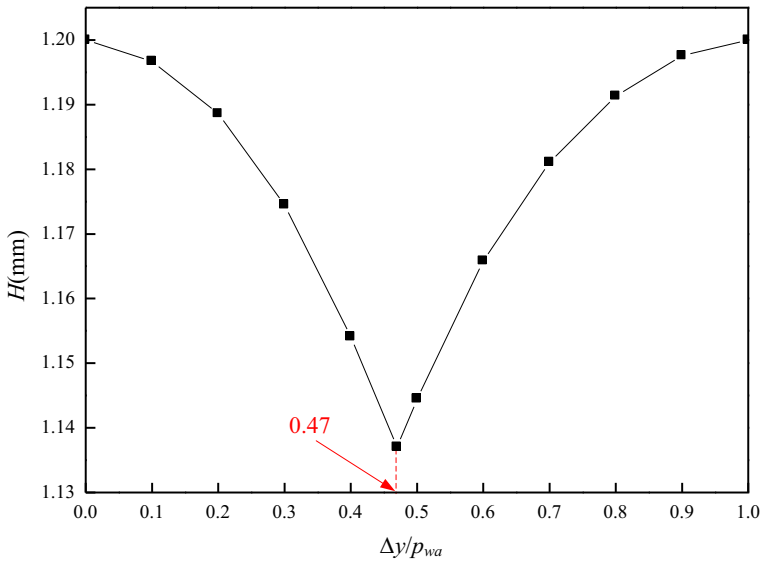
**Fig. 15** The change rule of total thickness $H$ with $\Delta y$

Figures 15 and 16 show the change rules of total thickness $H$ and through-thickness permeability $K_z$ with $\Delta y$. In those figures, the relative shift between the two unit-cells occurs only on $y$ direction, i.e. $\Delta x = 0$, $\Delta y \neq 0$, the shift period is $2p_{wa}$. As can be seen from the figures, the curves have the same pattern as Figs. 11 and 13, the total thickness and the through- thickness permeability reach the minimum values at $\Delta y = 0.47p_{wa}$ which is the maximum nesting position of $y$-shift.

It can be seen from the above analysis that a considerable degree of layer nesting occurs because of the unidirectional shift, for example, the total thickness of dual-layer EWR600 fabric decreases by up to 5~6%, and the through-thickness permeability decreases by up to 80%.
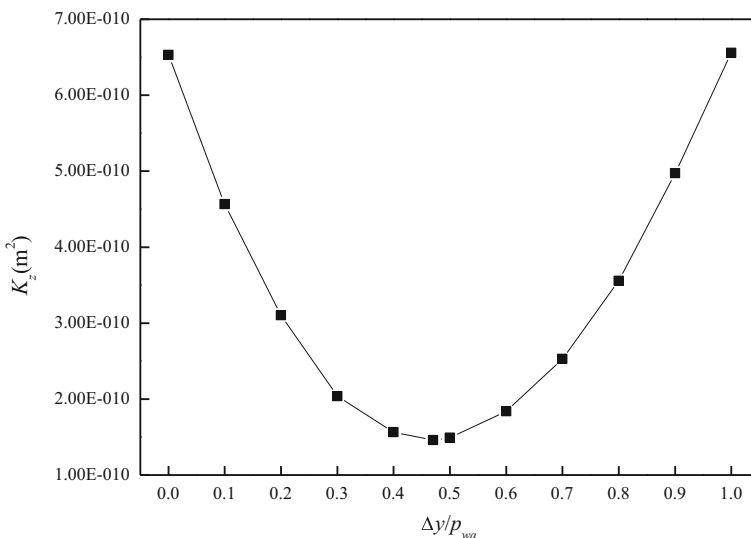


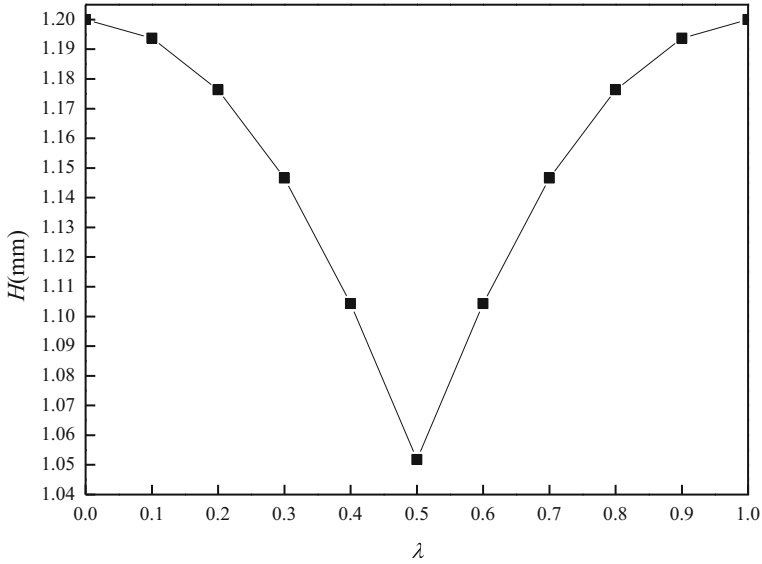**Fig. 16** The change rule of through-thickness permeability $K_z$ with $\Delta y$

**Fig. 17** The change rule of total thickness $H$ with $\lambda$

## 6.2 Bidirectional Shift

The bidirectional shift occurs when both the relative shift distances on $x$ and $y$ axis are not equal to 0, i.e. $\Delta x \neq 0$, $\Delta y \neq 0$. Let $\lambda = \Delta x/p_{we} = \Delta y/p_{wa}$, presented in Figs. 17 and 18 are the change rules of total thickness and through-thickness permeability of dual-layer EWR600 fabric with $\lambda$. When $\lambda = 1$, the relative position of the two layer fabric is identical to the initial position, that means the shift period of bidirectional shift is $\lambda = 1$, in a shift period, nesting behavior is symmetrical to $\lambda = 0.5$. According to the figures, we can find that the minimum
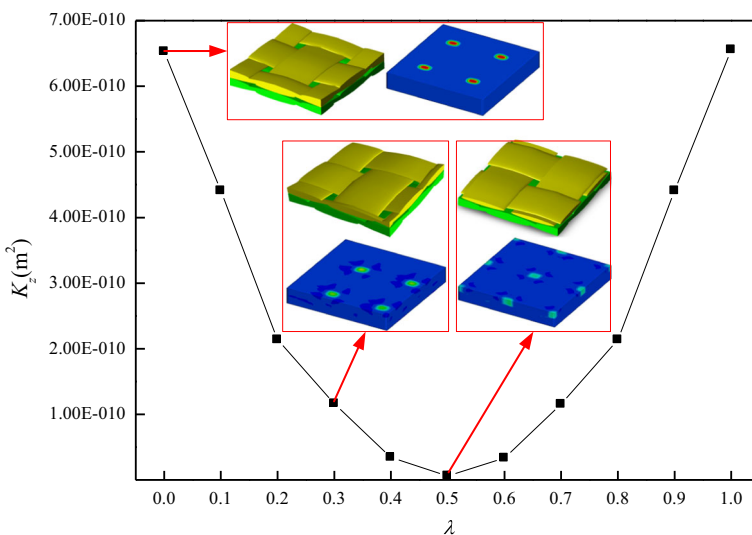


**Fig. 18** The change rule of through-thickness permeability $K_z$ with $\lambda$

total thickness and the minimum through-thickness permeability both appear at $\lambda = 0.5$, which means the maximum nesting position of bidirectional shift is the position of $\lambda = 0.5$.

Compared to the unidirectional shift, the bidirectional shift of fabric leads to a greater degree of nesting, the total thickness of dual-layer EWR600 fabric decreases more than 12%, and the through- thickness permeability is reduced more than two orders of magnitude.

# 7 Conclusions

Studying the through-thickness permeability of woven fabric has important implications for the through-thickness LCM processes, the layer nesting phenomenon of multilayer fabric has a great influence on the through-thickness permeability. In this article, the formation reason and characterization parameters of layer nesting were analyzed firstly, the geometry models of fabric unit-cells with different degrees of nesting were established based on ACIS. Then the through-thickness flow in the unit-cell of dual-layer fabric was analyzed and its mathematical model was built. The inter-yarn and intra-yarn regions of the unit-cell model were discretized uniformly, the through-thickness flow was numerically solved based on Adams-Bashforth scheme and Chorin projection method, and the through-thickness permeability of the fabric with nesting was predicted. The verification of the above method was checked by comparisons with the available experimental results. Finally, using EWR600 fabric as example, the effects of layer shift pattern on nesting behavior were studied, and the change rules of total thickness and through-thickness permeability with nesting degree were analyzed and discussed. It is found that compared to the length increase of the main flow channel, the width decrease is a more significant factor in reducing the through-thickness permeability. The results also show that a considerable degree of layer nesting may occur because of the unidirectional shift, the total thickness may decrease by up to 5~6%, and the reduction of through-thickness permeability may up to 80%. The bidirectional shift of fabric leads to a greater degree of nesting, the total thickness decreases more than 12%, and the through- thickness permeability decreases more than two orders of magnitude.

# References

1. Antonelli, D., Farina, A.: Resin transfer moulding: mathematical modelling and numerical simulations. Compos. Part A. **30**(12), 1367–1385 (1999)
2. Lam, Y.C., Joshi, S.C., Liu, X.L.: Numerical simulation of the mould-filling process in resin-transfer moulding. Compos. Sci. Technol. **60**, 845–855 (2000)
3. Belov, E.B., Lomov, S.V., Verpoest, I., Peters, T., Roose, D., Parnas, R.S., Hoes, K., Sol, H.: Modelling of permeability of textile reinforcements: lattice Boltzmann method. Compos. Sci. Technol. **64**, 1069–1080 (2004)
4. Kuentzer, N., Simacek, P., Advani, S.G., Walsh, S.: Permeability characterization of dual scale fibrous porous media. Compos. Part A. **37**, 2057–2068 (2006)
5. Louis, M., Huber, U.: Investigation of shearing effects on the permeability of woven fabrics and implementation into LCM simulation. Compos. Sci. Technol. **63**(14), 2081–2088 (2003)

6. Gokce, A., Advani, S.: Permeability estimation with the method of cells. J. Compos. Mater. **35**, 713–728 (2001)
7. Verleye, B., Croce, R., Griebel, M., Klitz, M., Lomov, S.V., Morren, G., Sol, H., Verpoest, I., Roose, D.: Permeability of textile reinforcements: simulation, influence of shear and validation. Compos. Sci. Technol. **68**, 2804–2810 (2008)
8. Zuo-Rong Chen, L., Ye, M.L.: Permeability predictions for woven fabric preforms. J. Compos. Mater. **44**(13), 1569–1586 (2010)
9. Drapiera, S., Monattea, J., Elbouazzaouia, O., Henrat, P.: Characterization of transient through- thickness permeabilities of non crimp new concept (NC2) multiaxial fabrics. Compos. Part A. **36**, 877–892 (2005)
10. Scholz, S., Gillespie Jr., J.W., Heider, D.: Measurement of transverse permeability using gaseous and liquid flow. Compos. Part A. **38**, 2034–2040 (2007)
11. Li, M., Wang, S.-K., Gu, Y.-Z., Li, Y.-X., Potter, K., Zhang, Z.-G.: Evaluation of through-thickness permeability and the capillary effect in vacuum assisted liquid molding process. Compos. Sci. Technol. **72**, 873–878 (2012)
12. Sas, H.S., Wurtzel, E.B., Simacek, P., Advani, S.G.: Effect of relative ply orientation on the through-thickness permeability of unidirectional fabrics. Compos. Sci. Technol. **96**, 116–121 (2014)
13. Yun, M., Carella, T., Simacek, P., Advani, S.: Stochastic modeling of through the thickness permeability variation in a fabric and its effect on void formation during vacuum assisted resin transfer molding. Compos. Sci. Technol. **149**, 100–107 (2017)
14. Markicevic, B., Papathanasiou, T.D.: An explicit physics-based model for the transverse permeability of multi-material dual porosity fibrous media. Transp. Porous Media. **53**, 265–280 (2003)
15. Xiao, X., Zeng, X., Long, A., Lin, H., Clifford, M., Saldaeva, E.: An analytical model for through-thickness permeability of woven fabric. Text. Res. J. **82**(5), 492–501 (2012)
16. Xiao, X., Endruweit, A., Zeng, X., Hu, J., Long, A.: Through-thickness permeability study of orthogonal and angle-interlock woven fabrics. J. Mater. Sci. **50**, 1257–1266 (2015)
17. Nabovati, A., Llewellin, E.W., Sousa, A.C.M.: Through-thickness permeability prediction of three-dimensional multifilament woven fabrics. Compos. Part A. **41**, 453–463 (2010)
18. Lomov, S.V., Verpoest, I., Peeters, T., Roose, D., Zako, M.: Nesting in textile laminates: geometrical modelling of the laminate. Compos. Sci. Technol. **63**(7), 993–1007 (2003)
19. Zeng, X., Endruweit, A., Brown, L.P., Long, A.C.: Numerical prediction of in-plane permeability for multilayer woven fabrics with manufacture- induced deformation. Compos. Part A. **77**, 266–274 (2015)
20. Hoes, K., Dinescu, D., Sol, H., Parnas, R.S., Lomov, S.: Study of nesting induced scatter of permeability values in layered reinforcement fabrics. Compos. Part A. **35**(12), 1407–1418 (2004)
21. Yang, B., Wang, S., Tang, Q.: Geometry modeling and permeability prediction for textile preforms with nesting in laminates. Polym. Compos. (2017). https://doi.org/10.1002/pc.24526
22. Fang, L., Jiang, J., Wang, J., Wang, J., Deng, C., Li, D., Liu, F.: Effect of layer shift on the out-of-plane permeability of 0°/90° noncrimp fabrics. J. Reinf. Plast. Compos. **33**(22), 2073–2094 (2014)
23. Fang, L., Jiang, J., Wang, J., Deng, C.: Effect of nesting on the out-of-plane permeability of unidirectional fabrics in resin transfer molding. Appl. Compos. Mater. **22**, 231–249 (2015)
24. Song, Y.S., Heider, D., Youn, J.R.: Statistical characteristics of out-of-plane permeability for plain-woven structure[J]. Polym. Compos. **30**(10), 1465–1472 (2010)
25. Yang, B., Jin, T., Zheng, L., Bo, Y., Jin, T., Long, Z.: Permeability prediction for textile preform with micro-meso dual-scale unit cell. Acta Materiae Compositae Sinica. **30**(5), 209–217 (2013). (In Chinese)
26. Gebart, B.R.: Permeability of unidirectional reinforcements for RTM. J. Compos. Mater. **26**, 1100–1133 (1992)
27. Guo, Y.W., He, Y.N.: Fully discrete finite element method based on second-order Crank-Nicolson/Adams-Bashforth scheme for the equations of motion of oldroyd fluids of order one. Discrete and Continuous Dynamical Systems-Series B. **20**(8), 2583–2609 (2015)
28. Xiao, X., Hu, J., Hua, T., Zeng, X., Long, A.: Through-thickness air permeability of woven fabric under low pressure compression. Text. Res. J. **85**(16), 1732–1742 (2015)
29. Dai, F., Zhang, B., Shanyi, D.: Permeability prediction of fabric preform using homogenization method. Acta Materiae Compositae Sinica. **26**(2), 90–93 (2009). (in Chinese)